

**ARTICLE**

## **History and Projection of Hydrological Droughts in the Benin Basin of the Niger River (Benin)**

**Yarou Halissou<sup>1,4\*</sup> Alamou Adéchina Eric<sup>2,4</sup> Biao Iboukoun Eliézer<sup>3,4</sup> Obada Ezéchiél<sup>2,4</sup>  
Tore Daniel Bio<sup>2,4</sup> Afouda Abel<sup>5,6</sup>**

1. International Chair of Mathematical Physics and Applications (ICMPA-UNESCO CHAIRE), University of Abomey-Calavi (UAC), Cotonou, Benin

2. National School of Public Works (ENSTP), National University of Sciences, Technologies, Engineering and Mathematics (UNSTIM), Abomey, Benin

3. National School of Mathematical Engineering and Modeling (ENSGMM), National University of Sciences, Technologies, Engineering and Mathematics (UNSTIM), Abomey, Benin

4. Laboratory of Environmental Geoscience and Application (LaGEA/UNSTIM), Benin

5. Applied Hydrology Laboratory (LHA), University of Abomey-Calavi (UAC), Cotonou, BP, 4521, Benin

6. West African Science Service Center on Climate Change and Adapted Land Use (WASCAL), GRP Climate Change and Water Resources, University of Abomey-Calavi (UAC), Abomey-Calavi, BP, 2008, Benin

---

**ARTICLE INFO**

*Article history*

Received: 2 April 2022

Revised: 5 May 2022

Accepted: 13 May 2022

Published: 20 May 2022

---

*Keywords:*

Hydrological

Drought

SDI

Beninese Niger river basin

---

**ABSTRACT**

In the context of a changing climate, the Beninese Niger River basin has been the focus of several research studies for the quantification, planning, and modeling of water and related resources for sustainable use. This research aims to characterize the historical (1976-2019) and projected (2021-2050) hydrological drought of the Beninese Niger River basin. The study used daily observations of rainfall, maximum and minimum temperatures, runoff rates and simulations of HIRHAM and REMO RCMs from fifteen (15) rainfall stations installed around the basin. It uses standardized streamflow indices (SDI) at 12-month and 36-month time steps. The results show that the calculated SDI indices show, on average, for all the model scenarios used, chronological trends of increase. These increases are not significant (are of the order of 0.00001 per year). The analysis of the SDI indices shows that, on average, the hydrological droughts in the Beninese basin of the Niger River will increase at 36 months and decrease at 12 months of the SDI. In fact, these small variations of hydrological droughts will be accompanied by the increase of their duration and the decrease of their magnitudes. The droughts detected in the Benin basin of the Niger River during the historical period will continue until 2050 in the same range but with more extended drought lengths. It should be noted that most of the changes observed in the calculated and analyzed indices are not significant.

---

\*Corresponding Author:

Yarou Halissou,

International Chair of Mathematical Physics and Applications (ICMPA-UNESCO CHAIRE), University of Abomey-Calavi (UAC), Cotonou, Benin; Laboratory of Environmental Geoscience and Application (LaGEA/UNSTIM), Benin;

Email: [halissou.yarou@gmail.com](mailto:halissou.yarou@gmail.com)

DOI: <https://doi.org/10.30564/jasr.v5i2.4602>

Copyright © 2022 by the author(s). Published by Bilingual Publishing Co. This is an open access article under the Creative Commons Attribution-NonCommercial 4.0 International (CC BY-NC 4.0) License. (<https://creativecommons.org/licenses/by-nc/4.0/>).

## 1. Introduction

The impacts of climate change and anthropogenic activities on water resources predicted by climatologists for the rest of the 21st century deserve special attention from mankind. The challenges of monitoring water resources, and in particular the anticipation of scarcity situations, nowadays require the implementation of specific operational hydrological applications, in the same way as those developed in recent years for flood forecasting<sup>[1]</sup>.

Extreme weather events usually have large impacts on society, water resources, health, and the agricultural sector<sup>[2]</sup>. A small change in average conditions can likely cause large changes for an extreme<sup>[2]</sup>. A better understanding of the statistical and physical nature of extreme climate events is a necessary step before we can answer questions that are related to these indices. It is important to note that each dry year involves significant socioeconomic losses and ecological damage worldwide<sup>[3]</sup>. Similarly, a very wet year results in socio-economic losses and damages.

The general problem of climate change is that, under projected climate scenarios, it would result in a higher frequency and intensity of extreme weather events<sup>[4]</sup>. These phenomena are even more accentuated in Africa where deforestation is very important<sup>[5]</sup>. The ministerial summit held in South Africa in 2007, which brought together 70 nations, recognized the magnitude of the drought problem and its impacts on food security and the sustainability of water resources, and emphasized the need for early warning systems for drought<sup>[6]</sup>.

The industrial revolution is to promote the impact of human activities on the environment that is becoming increasingly important, altering the climatic balance and thus having effects on precipitation. This phenomenon leads to drought. Drought is a normal and frequent feature of the climate. There are several types of drought<sup>[7]</sup>. Drought is defined from the meteorological, hydrological, agricultural or socio-economic point of view<sup>[8]</sup>. Drought does not have a universal definition. There are as many definitions of drought as there are water uses<sup>[7,9]</sup>. Hydrological drought is a decrease in water supply in streams, surface reservoirs, and groundwater. Hydrological drought is caused by a lack of precipitation accompanied by massive evaporation<sup>[10]</sup>. However, non-meteorological factors, such as water demand, availability of surface reservoirs, and artesian well drilling, compound the effect.

Since the second half of the 20th century, West Africa has been the region of the world with the largest rainfall deficit<sup>[11]</sup>. In Nigeria for example, a decreasing trend was observed in 98.2% of the landscape for the moisture index (MI), 96.7% for the SPI and 98.2% for the SPEI, showing

drying trends in the country<sup>[12]</sup>. Similarly in Niger, consecutive dry days have significantly increased and consecutive wet days have decreased. The same is true for rainy days. At the same time, the proportion of daily maximum rainfall in the annual rainfall total has increased over time and the proportion of intense rainfall in the annual rainfall total has significantly increased over the last two decades<sup>[13]</sup>. For Benin it is indicated for rainfall intensity and frequency indices such as consecutive rainy days and extremely wet day, respectively an increase and decrease<sup>[14]</sup>. For Kodja<sup>[15]</sup>, over the Oueme basin in Benin, there was a decreasing change in rainfall while the temperature velocity showed increasing changes for the period 1981-2010.

The Niger River has a hydrological regime that has evolved due to climate change and anthropogenic impacts. There are only a few dams on the Niger River, and future planned structures will alter its regime and flooded areas<sup>[16]</sup>. The Beninese basin of the Niger River, located in the semi-arid zone, is all the more affected as it records a significant demographic increase. This population growth intensifies the anthropic pressures on fragile resources whose degradation is increasingly worrying<sup>[17]</sup>. In order to highlight the dry sequences that have been little discussed so far in the Beninese basin of the Niger River and to assess their evolution in the near future in the said basin, the present work was interested in the study of standardized flow indices (SDI) at 12-month and 36-month intervals in the basin.

## 2. Methodology

### 2.1 Description of the Study Area and Data

The Beninese Niger River basin covers an area of approximately 48,000 km<sup>2</sup> (42% of the total area of Benin) and is located in the extreme north of Benin (Figure 1). Located between latitudes 10° and 12°30' north and longitudes 1°32' and 3°50' east, it includes the Mékrou, Alibori and Sota sub-basins, and is generally oriented SSW-NNE<sup>[18]</sup>. The implementation of this research work required the collection of several types of data. These are daily rainfall data observed from 1976 to 2019 at 15 rainfall stations (Figure 1) installed around the basin, which are collected from the Benin Meteorological Agency (Météo-Bénin); flow rate data which are extracted from the database of the Hydrology Department of the DGEau and concern the stations of Couberi and Gbassè on the Sota, Kompongou on the Mékrou and Yakin on the Alibori. These data cover the period from 1953-2017 (Coubéri and Yakin), 1953-2014 (Kompongou) and 1953-2006 (Gbassè); daily temperature observations (minimum and maximum) from three (03) synoptic stations (Figure 1) were considered. These data cover the period from 1976 to 2019. These data are com-

plemented by daily observations of radiation, wind speed and humidity for the calculation of daily ETP. It should be noted that data from the regional climate models DMI-HIRHAM5 (Denmark) and MPI-REMO (Germany) that have produced good results in the area [19] are used for the future period. These RCMs (Table 1) have a resolution of 50 km each and have been forced by GCM outputs (ECHAM5 for DMI-HIRHAM5 and MPI for MPI-REMO). These models have, at the daily scale for precipitation, historical simulations over the period 1960-2005 and simulations of RCP4.5 and 8.5 scenarios over the period 2006-2100. The future period selected is 2021-2050. For the observations, the period 1990-2019 was chosen from the historical period as the reference period for assessing changes.

## 2.2 Method Used

### 2.2.1 Calculation of SDI Indices

The SDI (Streamflow Drought Index) is a drought index based on streamflow. It is developed by Nalbantis and Tsakiris [22] based on the SPI method and calculations by replacing precipitation with streamflow.

If monthly streamflows  $Q_{i,j}$  of a time series are available, where  $i$  denotes the hydrological year and  $j$  denotes a month of that hydrological year ( $j=1$  for October and  $j=12$  for September),  $V_{i,k}$  can be obtained based on the equation:

$$V_{i,k} = \sum_{j=1}^{3k} Q_{i,j} \quad i = 1, 2, \dots, j = 1, 2, \dots, 12 \quad k = 1, 2, 3, 4 \quad (1)$$

where  $V_{i,k}$  is the cumulative flow rate for the  $i^{th}$  water year and  $k^{th}$  reference period,  $k=1$  for October-December,  $k=2$

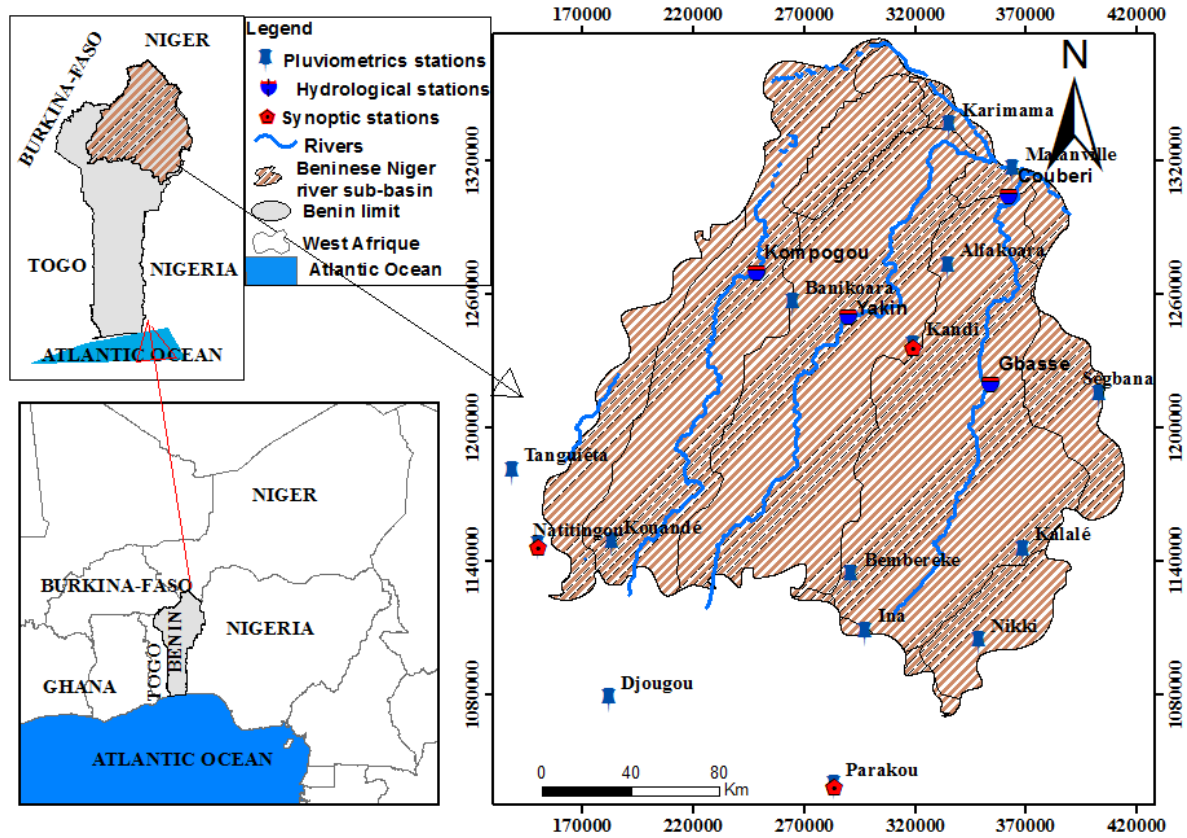


Figure 1. Location of the study stations.

Table 1. Characteristics of the regional climate models.

Model	Institution	Forcing MCG de	Horizontal resolution	Vertical level	Simulations	Reference
HIRHAM5	DMI	EC-EARTH	50 km	31	1951-2100	[20]
REMO	CSC	MPI-ESM-LR	50 km	27	1951-2100	[21]

for October-March,  $k=3$  for October-June and  $k=4$  for October-September.

Based on the cumulative flow rate,  $V_{i,k}$ , the flow drought index is given for each reference period  $k$  of the hydrological year  $i$  as follows:

$$SDI_{i,k} = \frac{V_{i,k} - \bar{V}_k}{S_k} \quad i = 1, 2, \dots, \quad k = 1, 2, 3, 4 \quad (2)$$

$V_k$  and  $S_k$  are the mean and standard deviation of the cumulative flow rates of the reference period  $k$  as determined for a long series.

As with the SPI, here too there are classes for the SDI. For this study, four (4) classes are considered (drought class) according to the SDI values. The values range from 1 (normal drought) to 4 (extreme drought) and are defined through the criteria in Table 2.

**Table 2.** SDI classes <sup>[22]</sup>

Classes	Description	Intervals
1	near-normal	$-0,99 \leq SDI < 0,99$
2	Moderate drought	$-1,49 \leq SDI < -1,0$
3	Severe drought	$-1,99 \leq SDI < -1,5$
4	Extreme drought	$SDI < -2,0$

Considering these four drought classes, the hydrological drought risk was estimated by the following formula:

$$RS_i = \frac{F_i}{F_T} * F_{ir} \quad (3)$$

$RS_i$ : hydrological drought risk of an event  $i$

$F_i$ : its Frequency

$F_{ir}$ : its rank considering the 10<sup>th</sup> percentile

$F_T$ : the total frequency.

$$RS = SPN + RM + RS + RE \quad (4)$$

$RS$ : the Risk of Hydrological Drought

$SPN = \sum RS_i$  of near-normal Hydrological Drought

$SM = \sum RS_i$  of Moderate Hydrological Drought

$SS = \sum RS_i$  Severe Hydrologic Drought

$SE = \sum RS_i$  Extreme Hydrologic Drought

### 2.2.2 Bias Correction

A bias correction is generally performed on climate model outputs for the majority of climate change impact studies. This correction is generally univariate and corrects each variable of interest independently of the others. There are a large number of bias correction methods. The bias correction method used in this research is called “Delta Change” (DC).

The DC method is the simplest and most widely used bias correction method <sup>[23-25]</sup> and consists of scaling the observations to obtain the corrected simulations. This is a modest method in which the parameters are typically corrected with a multiplicative or additive factor. In this

method, the factor at the scale of a period is applied to each incorrect daily observation of the same period to generate the corrected daily time series <sup>[26]</sup>. Equation (5) is used to correct for temperature and Equation (6) is used to correct for precipitation.

$$x_{cor,i} = x_{o,i} + \mu_p - \mu_b \quad (5)$$

$$x_{cor,i} = x_{o,i} \times \frac{\mu_p}{\mu_b} \quad (6)$$

where  $x_{cor,i}$  represents the corrected parameters;  $x_{o,i}$  represents the observed parameters.  $\mu_b$  and  $\mu_p$  are the average of the simulated data from the base period and the average of the data from the projection period, respectively.

In the present study, the Potential Evapotranspiration is calculated by the FAO Penman-Monteith <sup>[8]</sup> formula. This formula assumes: vegetation is a well-irrigated grass covering at a height of 0.12 m, external resistance of 70 s.m<sup>-1</sup> and an albedo of 0.23; daily heat flux into the soil is considered negligible in front of the net radiation at this time step ( $G \approx 0$ ); required climatic parameters: daily mean, maximum and minimum temperatures; daily mean air velocity at 2 m; daily total net radiation <sup>[27]</sup>. The formula is given by Equation (7).

$$ETP = \frac{0,408 \Delta R_n d + \gamma \left( \frac{900}{t+273} \right) v (e_w - e)}{\Delta + \gamma (1 + 0,34 v)} \quad (7)$$

$ETP$ : potential evapotranspiration (mm.d<sup>-1</sup>),  $R_n$ : net radiation (W.m<sup>-2</sup>),  $d$ : time step length in k seconds ( $d=0.0864$  ks),  $t$ : daily mean air temperature at 2m (°C),  $\Delta$ : slope of the saturating vapor pressure curve (kPa.°C<sup>-1</sup>),  $\gamma$ : psychrometric constant (kPa.°C<sup>-1</sup>),  $e$ : vapor pressure (kPa),  $e_w$ : saturation vapor pressure (kPa),  $v$ : wind speed at 2 m (m.s<sup>-1</sup>).

The parameters involved in the calculation of the Penman-Monteith daily ETP come from: i) direct field measurements for  $t_{mean}$ ,  $R_n$  and  $v$ ; ii) indirect measurements for  $e_w$  and  $e$  and iii) physical constants:  $\gamma$ ,  $\Delta$ .

The use of mean temperature underestimates  $e_w$ , the following expression is preferred:

$$e_w = \frac{e_w(t_{max}) + e_w(t_{min})}{2} \quad (8)$$

$e_w$ : saturation vapour pressure of the day (kPa);  $t_{max}$ : maximum temperature during the day (°C);  $t_{min}$ : minimum temperature during the day (°C)

$$e = \frac{e_w(t_{min}) \frac{Hr_{max}}{100} + e_w(t_{max}) \frac{Hr_{min}}{100}}{2} \quad (9)$$

$e$ : actual vapor pressure of the day (kPa);  $e_{w(tmax)}$ : saturation vapour pressure at the maximum daily temperature (kPa);  $e_{w(tmin)}$ : saturation vapour pressure at the minimum daily temperature (kPa);  $Hr_{max}$ : maximum relative humidity (%);  $Hr_{min}$ : minimum relative humidity (%).

$$\gamma = 0,665 \cdot 10^{-3} \cdot P \quad (10)$$

$\gamma$  in kPa.°C<sup>-1</sup>

$$P = 101,3 \cdot \left( \frac{293 - 0,0065 \cdot z}{293} \right)^{5,26} \quad (11)$$

$P$  in kPa,  $z$  the altitude in m.

$$\Delta = \frac{4098 \cdot \left[ 0,6108 \cdot \exp\left(\frac{17,27 \cdot t}{t+237,3}\right) \right]}{(t+237,3)^2} \quad (12)$$

$\Delta$  and kPa. °C<sup>-1</sup>,  $t$  and °C.

### 2.2.3 Assessment of Changes

Quantifying the effects of future changes in the extremes of daily climate variables is of great necessity to enable assessment of the vulnerability of hydrological systems to climate change.

In this study, future changes from the baseline period are evaluated using Equation (13). The 2021-2050 projection period was selected to assess changes in drought under the RCP4.5 and RCP8.5 scenarios of the REMO and HIRHAM climate models. A sub-period (1990-2019) was chosen as the reference period for assessing changes. This is to have the same length of series.

$$Change = \frac{\bar{x}_p - \bar{x}_r}{\bar{x}_r} \quad (13)$$

where  $\bar{x}_p$  is the average of the hydroclimatic parameter over the considered projection period and  $\bar{x}_r$  is its average over the reference period.

Student's t-test was applied on the hydrological parameters to assess the significance of the quantified changes.

### 2.2.4 Description of the Model Chosen for the Estimation of Flows (ModHyPMA)

The hydrological model ModHyPMA was used to model the flows of the rivers of the Beninese basin of the Niger River. It is a simple model and less constraining in terms of input data and gives good results. It does not use land use data, which makes it possible to make long-term projections. In addition, this model produces good results used on the Beninese basin of the Niger River by Gaba [28] and on the Mekrou River basin used by Obada [29]. Designed from the Least Action Principle, ModHyPMA (Hydrological Model based on the Least Action Principle) uses the principle of minimum energy expenditure. This principle can be stated as follows: "Nature always follows the simplest paths ... and the simplest paths are those that minimize nature's expenditure of energy" [30,31]. It is a physics-based, two-parameter, global hydrological model.

The ModHyPMA model includes a production function and a transfer function that are described by equations 4.49 and 4.50, respectively [31].

$$\frac{dZ(q,t)}{dt} = \Psi(q,t) \quad (14)$$

$$\frac{d(\lambda Q)}{dt} + vQ^{2v-1} = \Psi(q,t) \quad (15)$$

Equations (14) and (15) are an overall representation of the rainfall-flow transformation process.  $Q$  is the discharge at the watershed outlet,  $v$  is a nonlinearity parameter,  $\lambda$  is the basin drying coefficient,  $q$  is equal to the difference between rainfall and PTE all measured during a time  $t$ , and  $\Psi$  is a function. The scheme and main equations of the ModHyPMA are shown in Figure 2.

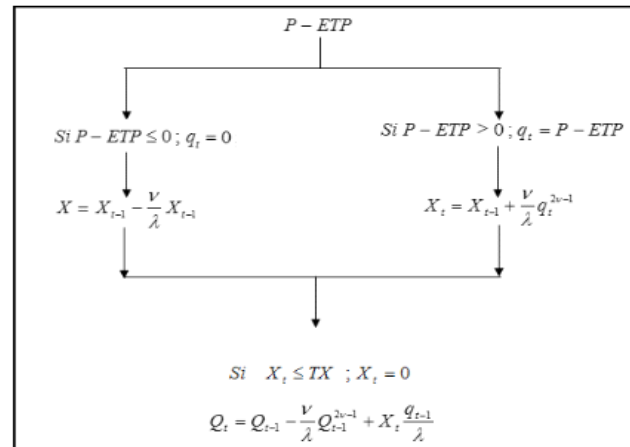


Figure 2. Schematic of the ModHyPMA model and key model equations [32,28,29].

- ✓ Step 1: The hydrological model ModHyPMA is calibrated for each watershed using the observed hydrological and climatic series.
- ✓ Step 2: The future climate series (2021-2050) are built from the observed series over a reference period of climate scenarios expressing a change in climate parameters.
- ✓ Step 3: The hydrological model with the parameters calculated in step 1 simulates the flows using the time series constructed in step 2.

## 3. Results

### 3.1 Analysis of the Performance of Bias Corrections on a Monthly Basis

Figures 3, 4 and 5 and Table 3 present the performance of the different results obtained from the method of corrections applied considering the annual averages of temperature and precipitation. On the one hand, these results show that the method (Delta) used to correct the data has been efficient. The table shows a large difference in the mean absolute error (MAE) between the raw data and the corrected data. The corrected data tend towards zero. On the other hand, we note that the method performs better with the temperature parameters than with the precipitation.

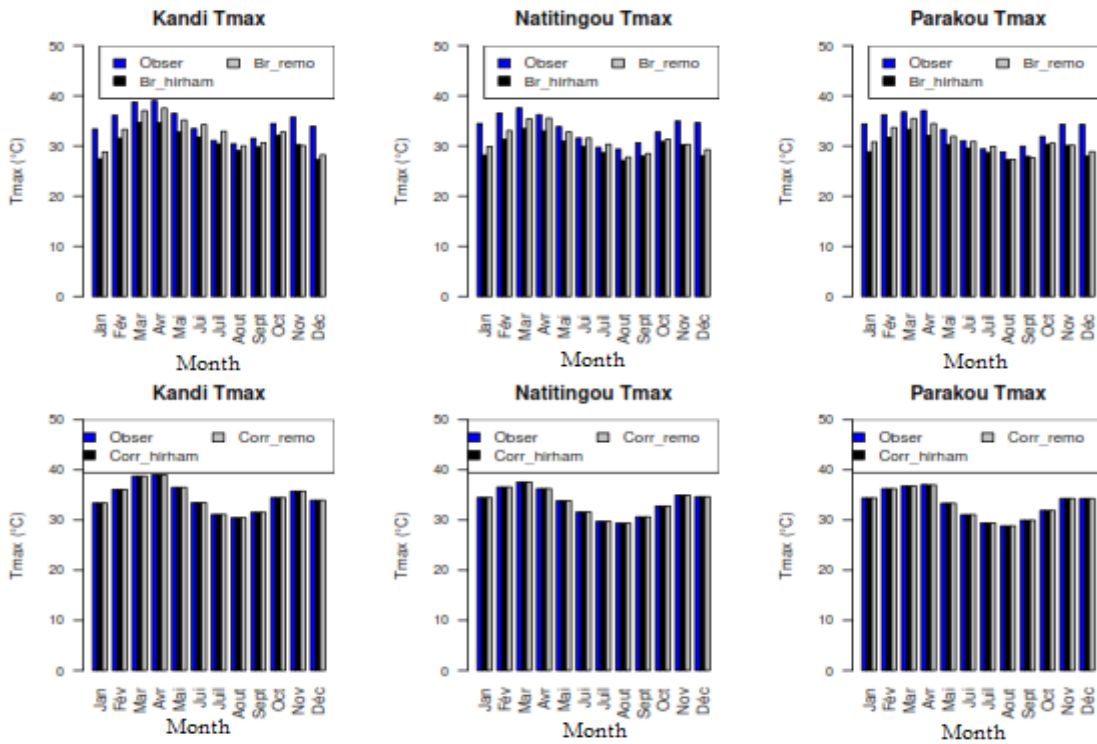


Figure 3. Performance of the correction method on annual temperature maxima (line 1 = raw data, line 2 = corrected data).

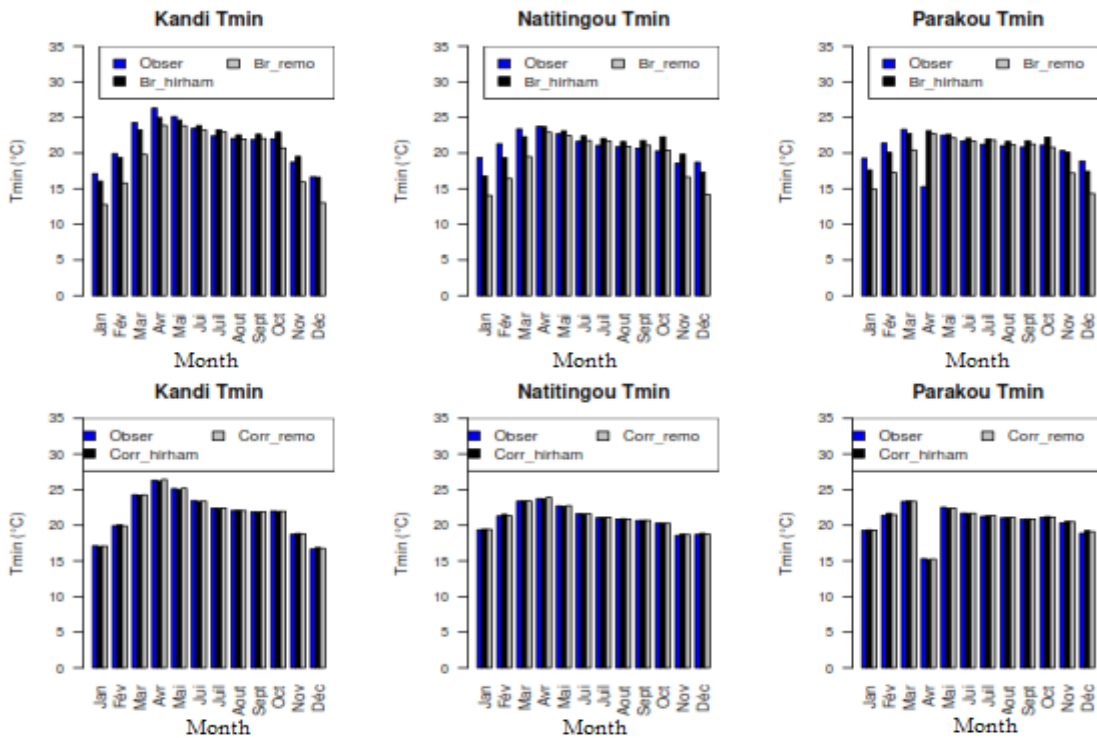


Figure 4. Performance of the correction method on annual temperature minima (line 1 = raw data, line 2 = corrected data).

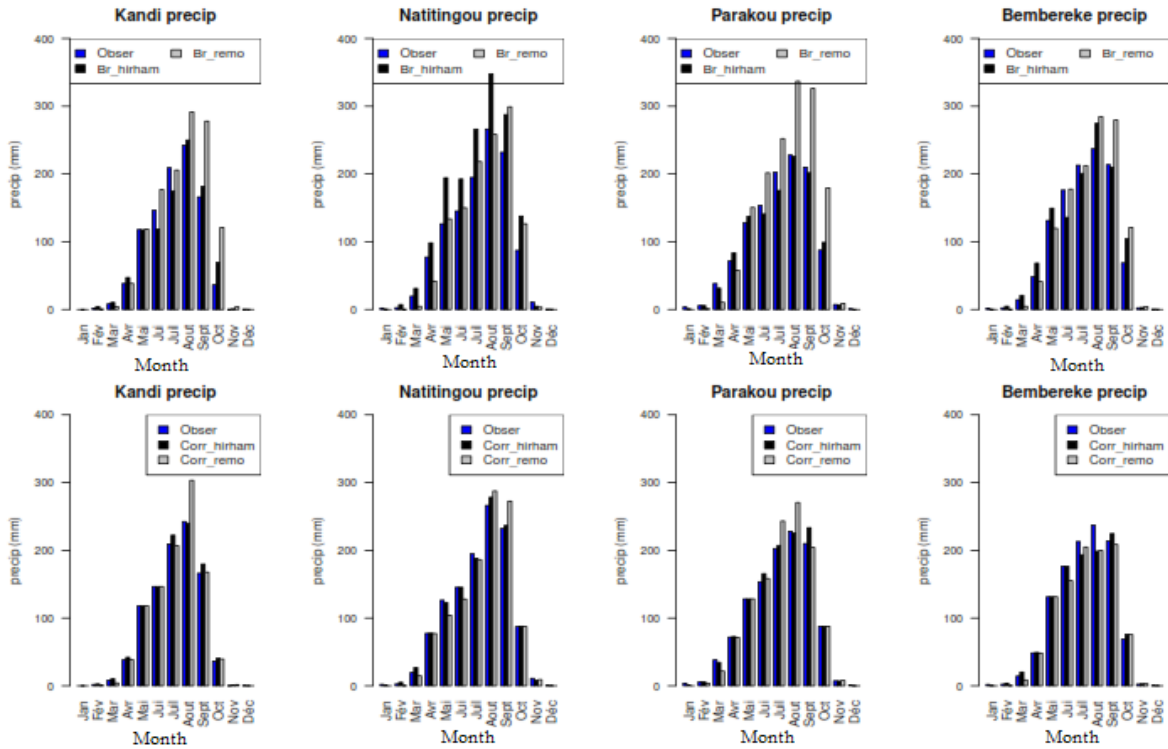


Figure 5. Performance of the correction method on annual rainfall (line 1 = raw data, line 2 = corrected data).

Table 3. Performance of the correction method on climate variables

Variables	Parameters	Station	Observation	Gross hirham	Corrected hirham	Gross remo	Corrected remo
Tmax	Deviation	Kandi	2,81	2,41	2,81	3,08	2,81
		Natitingou	2,74	2,04	2,74	2,50	2,74
		Parakou	2,88	1,85	2,87	2,56	2,87
	MAE	Kandi		3,55	0,00	2,41	0,00
		Natitingou		3,55	0,00	2,32	0,00
		Parakou		3,29	0,01	2,24	0,01
Tmin	Deviation	Kandi	3,05	3,01	2,96	4,17	3,04
		Natitingou	1,68	2,22	1,63	3,17	1,68
		Parakou	2,06	1,91	2,07	2,92	2,05
	MAE	Kandi		0,73	0,09	2,12	0,05
		Natitingou		1,19	0,08	1,91	0,05
		Parakou		1,41	0,13	2,36	0,08
Precipitation	Deviation	Kandi	90,62	86,34	92,62	112,13	101,57
		Natitingou	95,70	125,82	97,24	110,68	104,12
		Parakou	87,15	83,50	91,74	131,00	99,75
		Bembereke	95,44	96,38	89,26	111,79	88,15
	MAE	Kandi		11,06	3,37	24,19	6,26
		Natitingou		34,96	3,54	17,71	10,20
		Parakou		7,79	4,28	40,87	9,88
		Bembereke		14,92	7,19	16,91	7,49

### 3.2 Flow Simulation and Hydrological Model Performance

The performance of the ModHyPMA model in calibration and validation at each hydrometric station is sum-

marized in Table 4. Figure 6 presents the values of Nash criteria and coefficients of determination ( $R^2$ ) in calibration and validation for the hydrological stations used. The analysis of the table and the figure shows that during

calibration, the model responded well at all hydrological stations. Indeed, the results show Nash criteria values and coefficients of determination higher than 50% in calibration as in validation. The hydrographs of observed and simulated flows of the ModHypMA model at each station are shown in Figure 7.

**Table 4.** Performance of the ModHypMA model at each station.

		Gbasse	Couberi	Kompongou	Yakin
Calibration	Year	1986-1990	1986-1989	1971-1974	1984-1987
	X1	1,142	1,0785	1,0114	1,24
	X2	46,313	68,923	35,322	67,883
	R <sup>2</sup>	0,775	0,701	0,871	0,571
	Nash	0,639	0,684	0,767	0,594
Validation	Year	2003-2006	2003-2007	2007-2010	2005-2008
	X1	1,142	1,0785	1,0114	1,24
	X2	46,313	68,923	35,322	67,883
	R <sup>2</sup>	0,635	0,678	0,621	0,557
	Nash	0,59	0,738	0,551	0,534

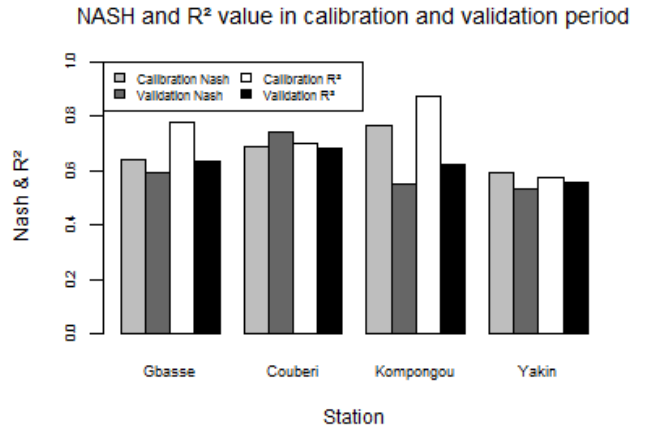


**Figure 6.** NASH criterion values and coefficient of determination by hydrologic station.

### 3.3 Analysis of Historical Hydrological Droughts

Figure 8 shows the chronological evolution of the SDI indices at each hydrological station during the period 1976-2019. From this figure, it can be seen that at the

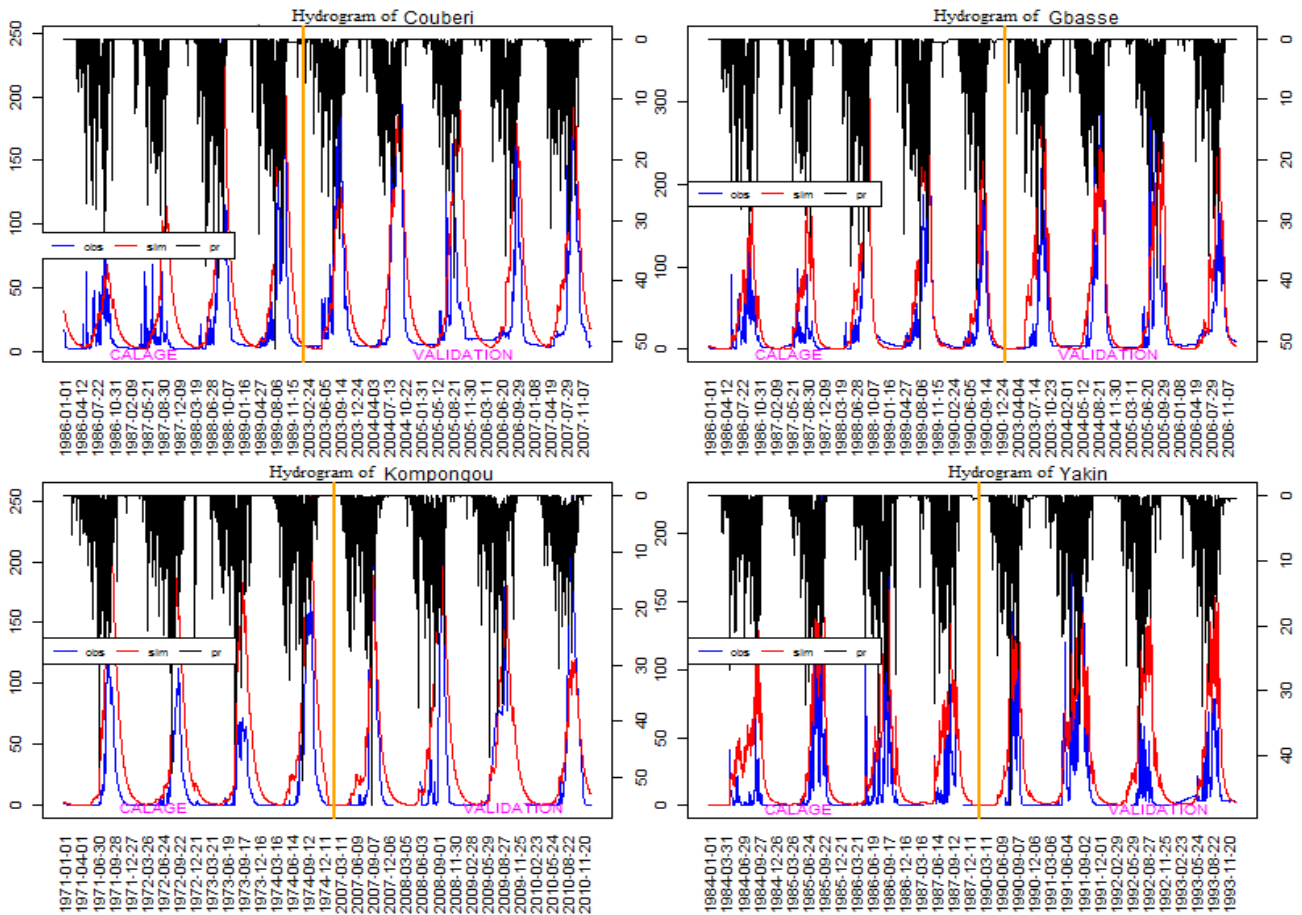


**Figure 7.** Results of the ModHypMA model in calibration and validation by hydrological station.

Couberi hydrometric station, the index shows an average increasing trend of 0.0001 per year for the SDI-12 and SDI-36 months. It is also noted that the major dry periods are located between the years 1978-1988. At this station, at the 12-month SDI scale, extreme drought occurred in 1.4% of the cases, severe drought in 12.83% of the cases, moderate drought in 8.72% of the cases, and near-normal conditions 77% of the cases (Figure 9). For the 36-month IDS, we observed 73.87%, 18.67%, 5.07% and 1.4% of near-normal, moderate, severe and extreme conditions respectively (Figure 9). Through Figure 10 we notice that the average duration of drought at this station is 21 months with a peak of  $-1.68$  for the SDI-12 months against 85 months of duration and  $-2.2$  of peak for the SDI-36 months. At Couberi, we also note that at 12 months SDI, there is a greater chance (36%) of hydrological drought than at 36 months SDI (30%) (Figure 11).

In Gbassè, at the 12-month IDS scale, the frequencies of 80.25%, 13.13%, and 6.22% for near-normal, moderate, and severe conditions, respectively, were noted during the reference period (Figure 9). Extreme droughts did not occur. At 36 months IDS, at this station, near-normal, moderate and severe conditions show 76.81%, 17.71% and 5.49% respectively with an absence of extreme droughts (Figure 9). The two calculated SDI windows show very small time series decreases (averaging 1/100000 per year) over the selected historical period (Figure 8). The droughts are localized between 1978-1988 and 2010-2019 (Figure 8). Furthermore, drought duration range up to 47 and 117 months respectively for SDI-12 and SDI-

36 months with respective peaks of  $-1.6$  and  $-1.8$  (Figure 10). As in Couberi, here too the risk of drought is higher at 12 months IDS than at 36 months (Figure 11).

At the 12-month and 36-month SDI scale, 80.24% and 81.28% of near-normal droughts; 5.23% and 9.25% of moderate droughts; 9.03% and 5.1% of severe droughts; and 4.51% and 5.57% of extreme droughts are identified at the Kompongou station respectively (Figure 9). These SDI windows (12 months and 36 months) calculated at the Kompongou station all show non-significant increasing time trends (Figure 8). This increase is on average 5/100,000 per year (Figure 8). This station shows its dry periods between 1978-1988 and 2010-2019 (Figure 8). On average, there are 36 months and 117 months of drought duration respectively with SDI-12 and SDI-36 months associated with peaks of  $-2.12$  and  $-2.75$  (Figure 10). Unlike the previous stations, here the risk of drought is higher with SDI-36 (46.11%) months than with SDI-12 (38.38%) months (Figure 11).

At the Yakin hydrometric station, the extreme drought did not occur for all the SDI steps as at Gbassè (Figure 9). For this station, 80.75% of near-normal conditions, 12.5% of moderate drought and 6.25% of severe drought were noted for the SDI-12 months, compared to 79.33% of near-normal drought, 12.927% of moderate drought and 7.75% of severe drought for the SDI-36 months (Figure 9). On average, drought duration is up to 24 months for the SDI-12 months and 48 months for SDI-36 months with respective peaks of  $-1.64$  and  $-1.6$  (Figure 10). The SDI-12 months is increasing over time by 0.007 (very low) per

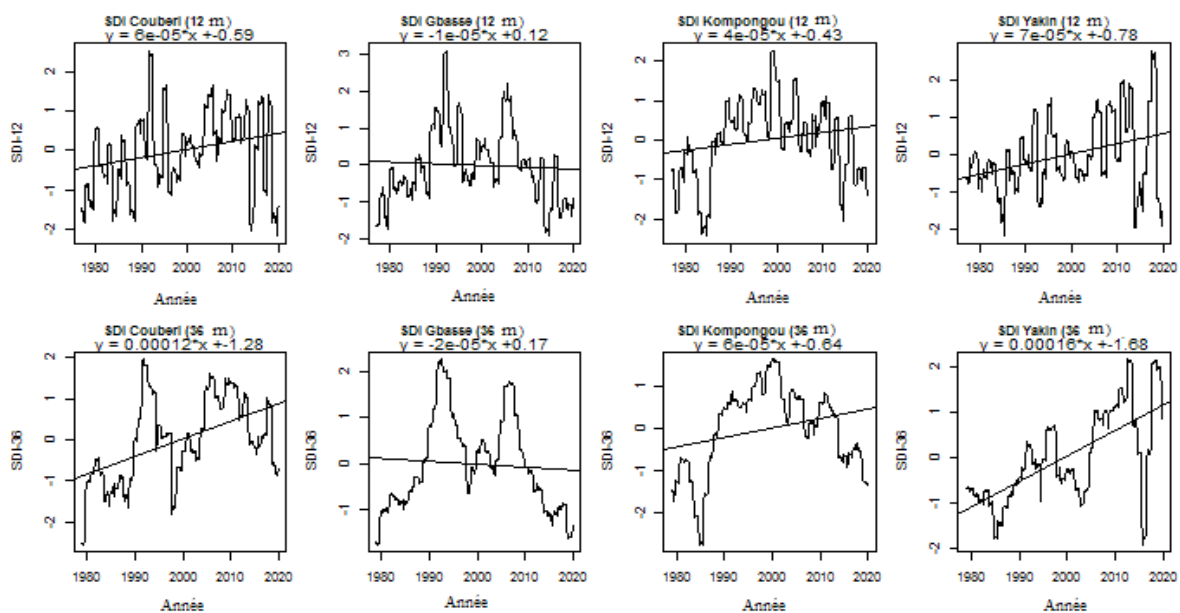


Figure 8. Chronological evolution of SDI indices by hydrological station.

centennial while the SDI-36 months is increasing over time by 0.01 (very low) per centennial (Figure 8). As in Kompongou, in Yakin, we note that at 36 months SDI the risk of drought (which is 29%) is higher than at 12 months SDI (where we have 28%) (Figure 11).

In sum, for all the hydrometric stations considered for the calculation of the SDI, it can be seen that at the 12-month and 36-month scales of the SDI, the frequencies of conditions close to normal drought prevail over

the other drought classes (Figure 9). At these IDS scales, extreme droughts always come last while moderate and severe droughts are second and third respectively. The hydrological drought risks calculated at each SDI window (12 months and 36 months) show us that the Kompongou station is the one where the hydrological drought risks are high for all SDI windows. This is followed by Couberi, Yakin and Gbassè stations respectively (Figure 11).

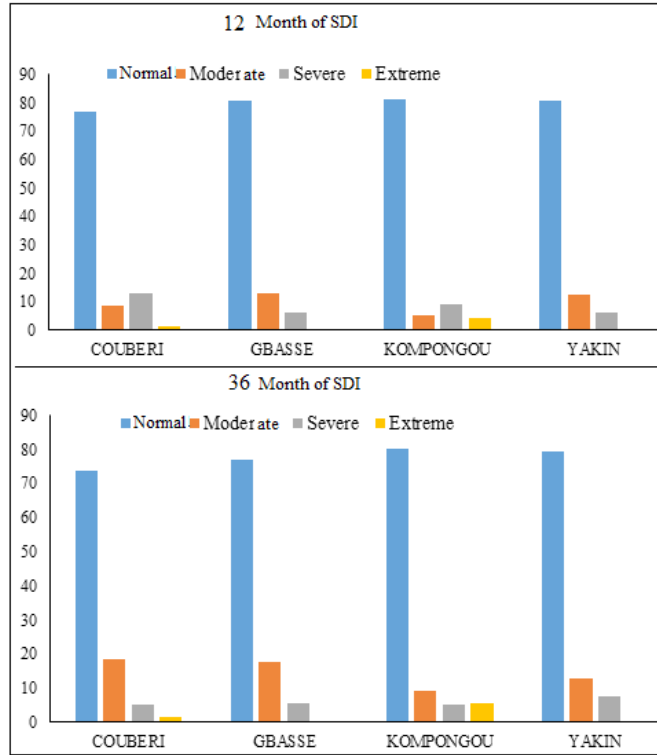


Figure 9. Occurrence of drought classes at each hydrological station.

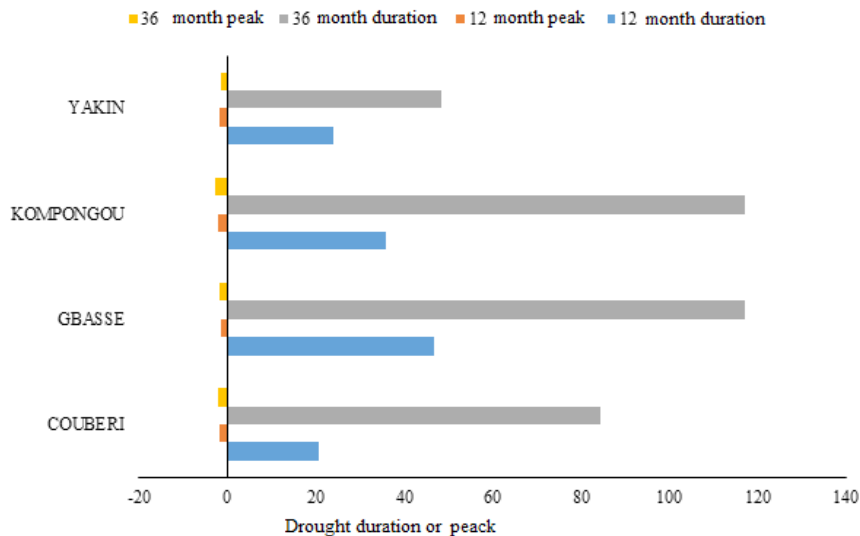


Figure 10. Drought duration and peaks by hydrological station.

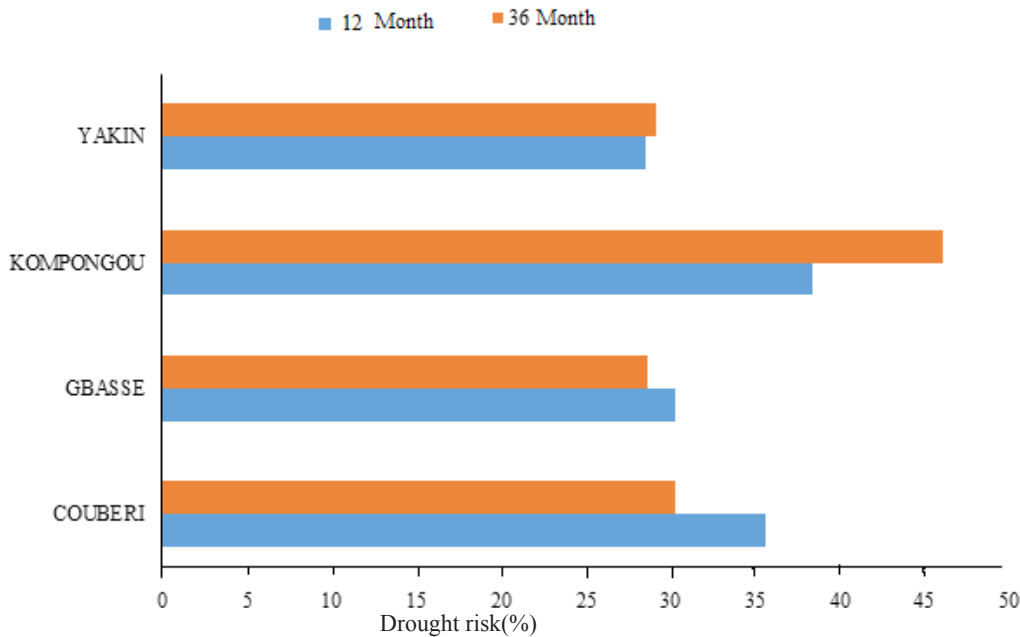


Figure 11. Drought risk by hydrological station.

### 3.4 Analysis of Projected Hydrological Droughts (2021-2050)

Both scenarios (RCP4.5 and RCP8.5) of the two models (HIRAHM and REMO) show at Couberri for the medium term, increasing time trends in normalized flow indices except for HIRHAM's RCP4.5 for the SDI-36month (Figures 12 and 13). These increases are very small (1/100000 per year) (Figures 12 and 13). At Gbassè, Kompongou and Yakin, the scenarios also show medium-term trends of increasing indices, except for HIRHAM's RCP4.5, which shows decreases for both indices at these stations (Figures 12 and 13). For all of these stations and for the 12 and 36 month SDI, the variations are very small (1/100,000 per year) (12 and 13). Except for Gbassè, where these trends were downward in the past, the other stations showed upward trends with variations that are in the same order.

On average for all hydrological stations during the period 2021-2050 and for the SDI-12 months, we note for the RCP4.5 of the HIRHAM, 80%, 11%, 7% and 1% respectively of near-normal, moderate, severe and extreme droughts. While with the RCP8.5 of the same model the values are respectively 77%, 14%, 8% and 1%. On the other hand, with the REMO model, the RCP4.5 gives 79%, 14%, 5% and 2% of near-normal, moderate, severe and extreme droughts respectively, while its RCP8.5 gives 74%, 21%, 4% and 1% respectively (Figure 14). During the reference period, 78%, 13%, 6% and 3% of near-normal, moderate, severe and extreme droughts were recorded for the 12-month IDS, respectively. At 36 months of the IDS and in the near future, the HIRHAM RCP4.5

shows 77%, 10%, 9% and 4% respectively of near-normal, moderate, severe and extreme droughts against 80%, 11%, 5% and 3% respectively for the RCP8.5 of the same model. The REMO model presents through the RCP4.5 respectively 78%, 10%, 7% and 5% of droughts close to normal, moderate, severe and extreme while through its RCP8.5 we note respectively 81%, 11%, 4% and 4% (Figure 15). In the past, 76%, 16%, 5% and 3% of droughts were near-normal, moderate, severe and extreme respectively. For all models and SDI steps, near-normal drought prevails in about 75% of the drought cases (Figures 14 and 15). In the past, 76%, 16%, 5%, and 3% of near-normal, moderate, severe, and extreme droughts were observed for the SDI-36 months, respectively.

For the drought duration in the medium term (2021-2050), for the 12-month SDI, with RCP4.5 of the HIRHAM model, average drought duration of 24 months, 19 months, 21 months and 22 months are recorded with respective peaks of -1.72, -1.65, -1.76 and -1.77 at Couberri, Gbassè, Kompongou and Yakin respectively (Figure 16). With RCP8.5 of the same model, these duration are respectively 18 months, 11 months, 12 months and 10 months associated with peaks of -1.67, -1.58, -1.57 and -1.64 (Figure 16). On the other hand, with REMO's RCP4.5, the duration for the near future are 31 months, 24 months, 24 months and 23 months with peaks of -1.76, -1.61, -1.66 and -1.7 respectively for the Couberri, Gbassè, Kompongou and Yakin stations, compared to duration of 22 months, 23 months, 18 months and 15 months and peaks of -1.43, -1.41, -1.48 and -1.4 for the RCP8.5 of the same model (Figure 16). During the baseline peri-

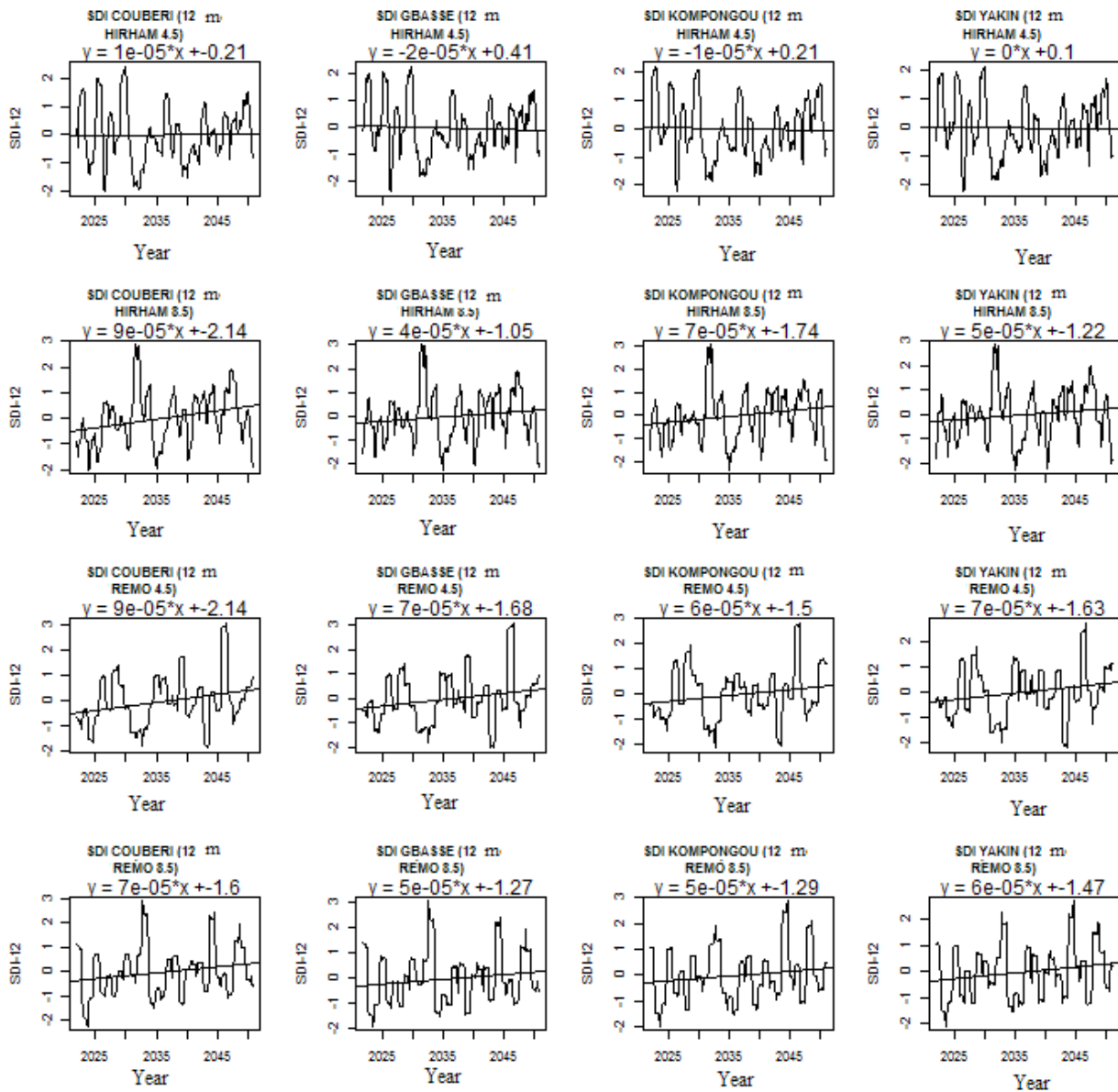


Figure 12. Projected 12-month SDI trends by hydrologic station (2021-2050).

od, drought duration of 21 months, 47 months, 36 months and 24 months was recorded at Couber, Gbassè, Kompongou and Yakin respectively with peaks of  $-1.63$ ,  $-1.57$ ,  $-2.12$  and  $-1.64$ . At 36 months from the SDI, the RCP4.5 of the HIRHAM model shows for the near future, drought duration of 45 months, 46 months, 56 months and 45 months respectively in Couber, Gbassè, Kompongou and Yakin with respective peaks of  $-2.3$ ,  $-2.2$ ,  $-2.2$  and  $-2.2$  while its RCP8.5 shows respective duration of 33 months, 31 months, 42 months and 33 months with peaks of  $-1.75$ ,  $-1.71$ ,  $-1.8$  and  $-1.7$  (Figure 17). For the RCP4.5 of the REMO model, at 36 months from the SDI and in the near future, we have drought duration of 46 months, 34 months, 42 months and 31 months with respective peaks

of  $-2$ ,  $-1.6$ ,  $-2$  and  $-1.8$  at Couber, Gbassè, Kompongou and Yakin. With its RCP8.5, these stations have duration of 37 months, 51 months, 26 months and 21 months respectively with peaks of  $-1.7$ ,  $-1.8$ ,  $-1.6$  and  $-1.7$  (Figure 17). During the historical period, drought duration of 85 months, 117 months, 117 months and 48 months were observed at Couber, Gbassè, Kompongou and Yakin respectively, with peaks of  $-2.17$ ,  $-1.75$ ,  $-2.75$  and  $-1.59$ .

The two scenarios (RCP4.5 and RCP8.5) of the two models (HIRHAM and REMO) present on average 34% and 36% risk of hydrological drought for the study basin with SDI-12 and SDI-36 months respectively. In the past, these risks were estimated at 33% and 34% months respectively.

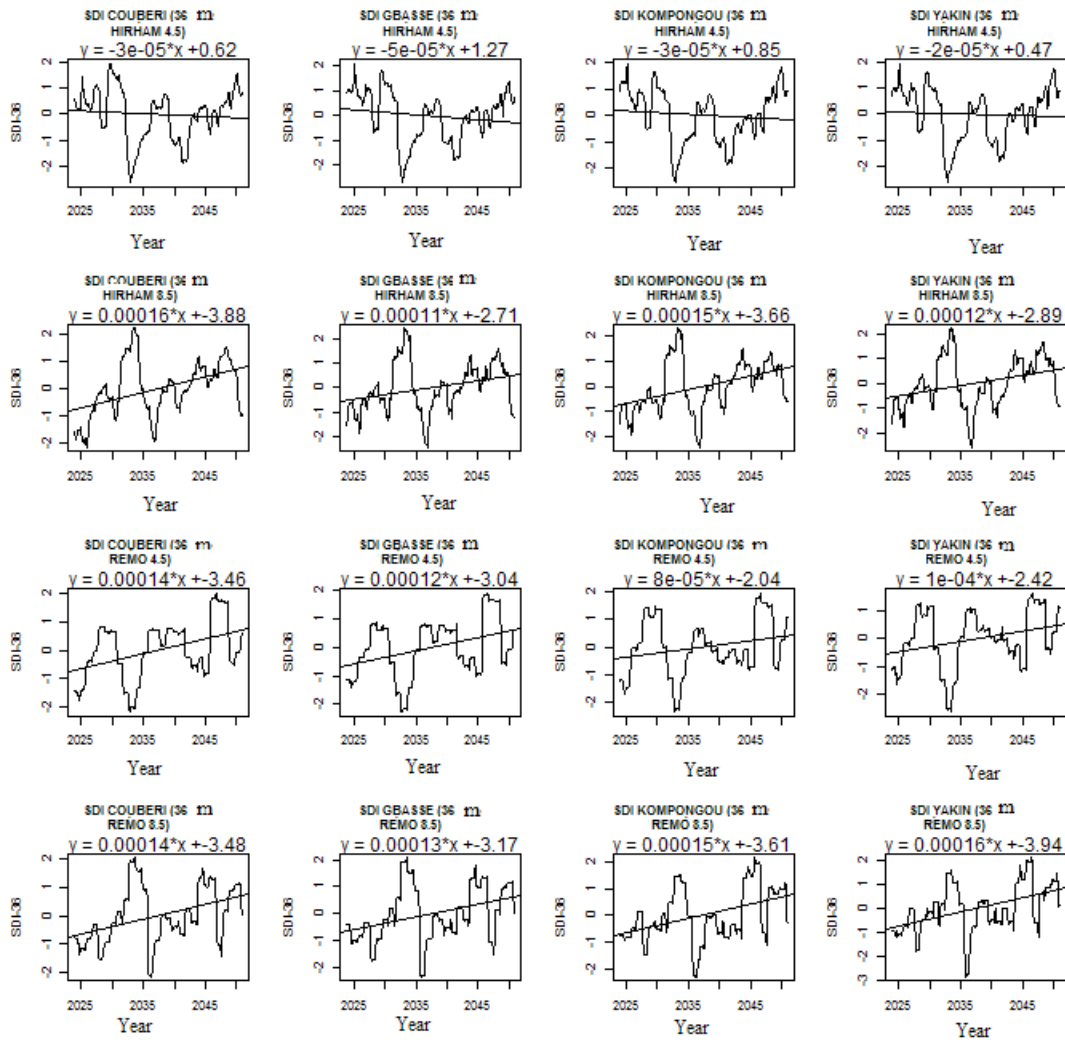


Figure 13. Projected 36-month SDI trends by hydrologic station (2021-2050).

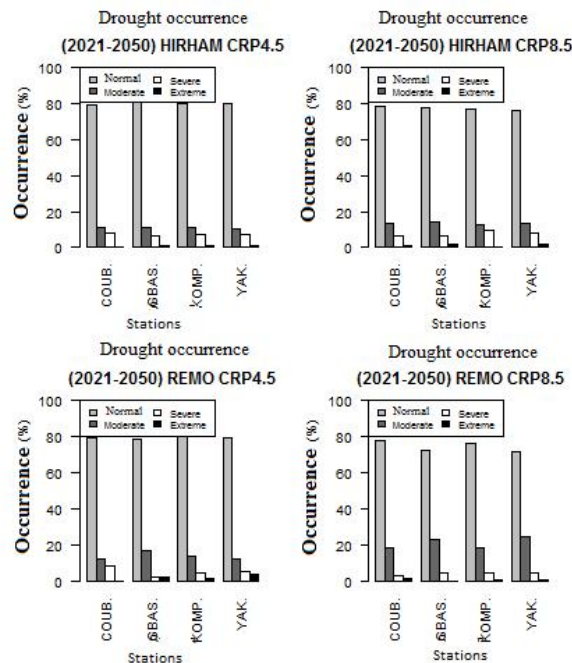


Figure 14. Projected drought class occurrences for each hydrologic station for the 12-month SDI (2021-2050).

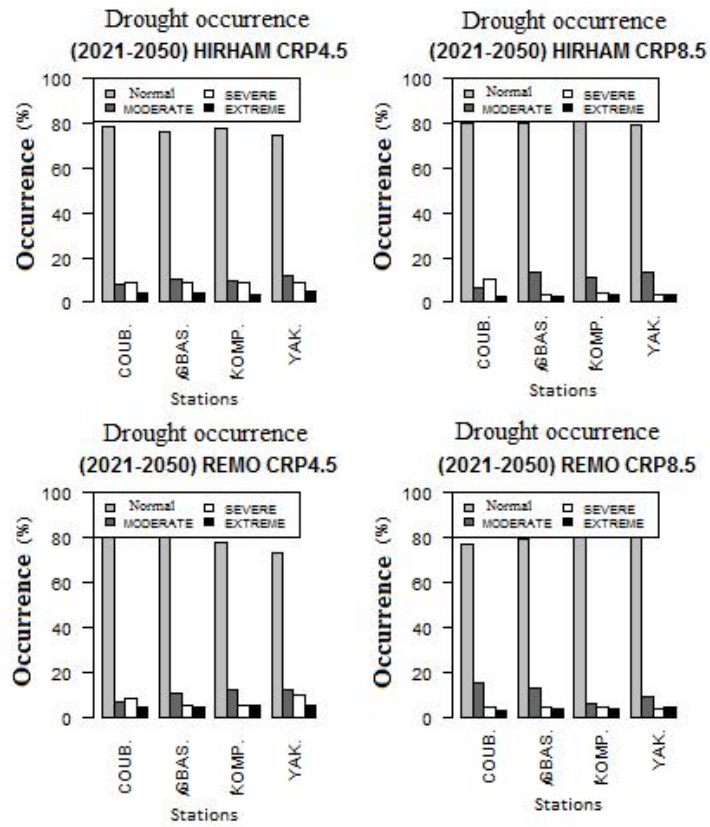


Figure 15. Projected drought class occurrences for each hydrologic station for the 36-month SDI (2021-2050).

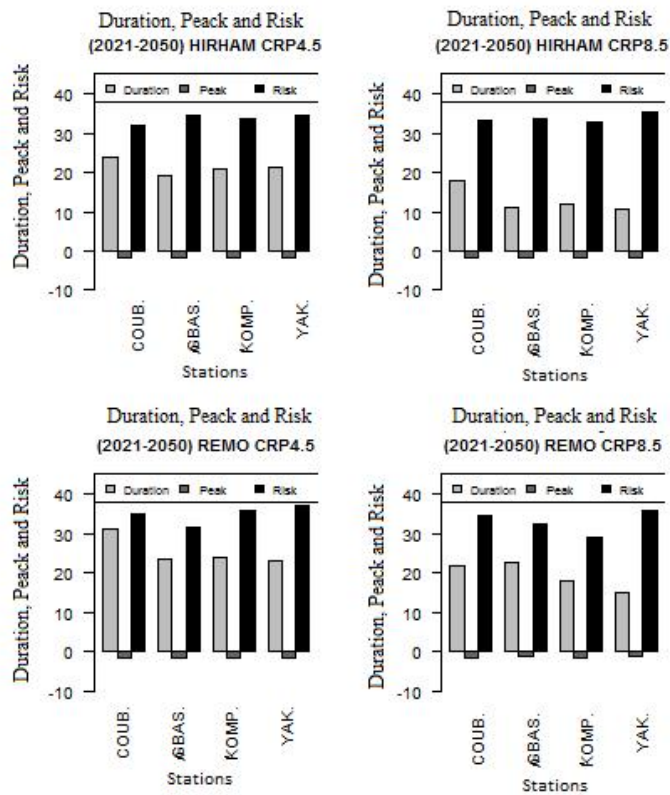


Figure 16. Projected duration, peaks, and risks for all hydrologic stations at the 12-month IDS scale (2021-2050).

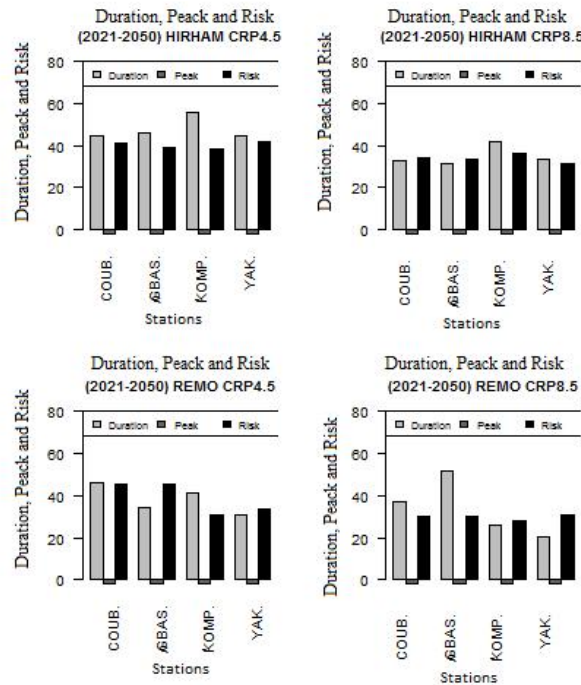


Figure 17. Projected duration, peaks, and risks for all hydrologic stations at the 36-month IDS scale (2021-2050).

### 3.5 Evaluation of Changes

In the study basin, in the medium term and for the SDI-12 months, we note on average through Figure 18 the decrease in moderate and extreme droughts and the increase in near-normal and severe droughts compared to the reference period according to HIRHAM’s RCP4.5. In fact, we record  $-1.8\%$ ,  $-1.6\%$ ,  $2.1\%$  and  $1.3\%$  respectively for these drought classes. With the HIRHAM RCP8.5, we note the decrease in near-normal and extreme droughts and the increase in moderate and severe droughts compared to the reference period (Figure 18). The rates for these drought types are  $-0.77\%$ ,  $-1.45\%$ ,  $0.5\%$  and  $1.69\%$  respectively. REMO’s RCP4.5, in the medium term and for the SDI-12 months, shows deviations of  $1.35$ ,  $0.64$ ,  $-1.14$  and  $-0.85$  respectively for near-normal, moderate, severe and extreme droughts compared to the baseline period (Figure 18). During the same period and for the same SDI step, REMO’s RCP8.5 shows for near-normal, moderate, severe and extreme droughts respective deviations of  $-3.57\%$ ,  $7.95\%$ ,  $-2.15\%$  and  $-2.22\%$  from the baseline period (Figure 18).

In the medium term and for the SDI-36 months, there is a decrease in moderate droughts and an increase in near-normal, severe and extreme droughts compared to the reference period according to HIRHAM RCP4.5 (Figure 18). For these drought classes, there are deviations of  $-0.67\%$ ,  $-5.79\%$ ,  $3.97\%$  and  $1.15\%$  respectively. With the HIRHAM RCP8.5, we observe a decrease in

moderate and severe droughts and an increase in near-normal and extreme droughts compared to the reference period (Figure 18). For these drought types, the rates are  $-4.53\%$ ,  $-0.07\%$ ,  $4.01\%$  and  $0.58\%$ , respectively. REMO’s RCP4.5, in the medium term and for the SDI-36 months shows deviations of  $1.76\%$ ,  $-5.19\%$ ,  $1.97\%$  and  $1.46\%$  respectively for near-normal, moderate, severe and extreme droughts compared to the baseline period (Figure 18). During the same period and for the same IDS step, REMO’s RCP8.5 shows for near-normal, moderate, severe and extreme droughts respective deviations of  $5.25\%$ ,  $-4.96\%$ ,  $-0.61\%$  and  $0.32\%$  from the baseline period (Figure 18).

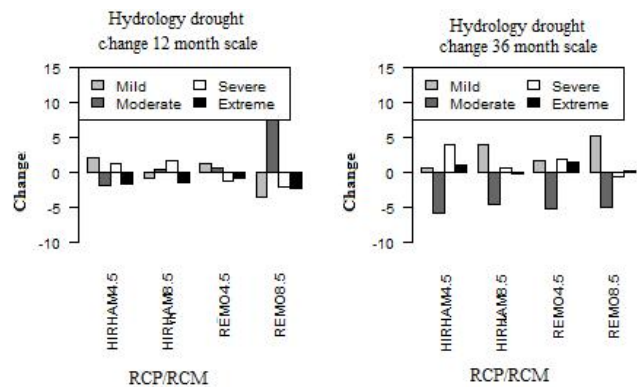


Figure 18. Change in drought types between the baseline and projection periods (12 and 36 month IDS scale).

At the 12-month step of the SDI, we note decreases

in drought duration with the HIRHAM RCP8.5 at all stations, while peaks increase at Kompongou and Yakin and decrease at Couberi and Gbassè (Figure 19). These decreases in duration are 1.95 months, 7.28 months, 6.25 months and 19.06 months respectively at Couberi, Gbassè, Kompongou and Yakin relative to the baseline period with respective peak deviations of  $-0.08$ ,  $-0.03$ ,  $0.49$  and  $0.9$  relative to the baseline period (Figure 19). For RCP4.5 of the same model, we note increases of 4 months, 0.7 months and 2.75 months respectively at Couberi, Gbassè and Kompongou with respective peak deviations of  $-0.13$ ,  $-0.1$  and  $0.3$  and a decrease of 8 months at Yakin with a peak deviation of  $-0.04$  with respect to the baseline period (Figure 19). REMO's RCP4.5 shows increases of 11.58 months, 5 months and 6 months respectively in Couberi, Gbassè and Kompongou with respective peak differences of  $-0.16$ ,  $-0.06$  and  $0.39$  compared to the reference period and a decrease of 6.5 months in Yakin with a peak difference of  $0.04$  (Figure 19). In contrast, its RCP8.5 shows a decrease of 14.5 months at Yakin with a peak difference of  $0.31$  and increases of 1.85 months, 4.1 months and 0

month respectively at Couberi, Gbassè and Kompongou with respective peak differences of  $0.16$ ,  $0.14$  and  $0.57$  from the baseline period (Figure 19).

In the medium term and at 36 months from the SDI, we note increases in drought duration and decreases in peaks with HIRHAM's RCP4.5 at Gbassè, Kompongou and Yakin, while the opposite is noted at Couberi (Figure 20). These increases in duration are 46 months, 56 months, and 4.8 months respectively, associated with decreases in duration gaps of 2.23, 2.2, and 0.43 respectively at Gbassè, Kompongou, and Yakin compared to the baseline period, compared to a duration gap of  $-38.5$  months and a peak gap of  $0.35$  at Couberi (Figure 20). For RCP8.5 of the same model, we note drought duration deviations of  $-50.33$  months, 31.25 months, 41.66 months and  $-6.42$  months respectively at Couberi, Gbassè, Kompongou and Yakin with respective peak deviations of  $0.85$ ,  $-1.72$ ,  $-1.8$  and  $0.07$  compared to the baseline period (Figure 20). REMO's RCP4.5 shows differences in drought duration of  $-31$  months, 34.33 months, 41.5 months and 8.67 months respectively at Couberi, Gbassè, Kompongou and Yakin

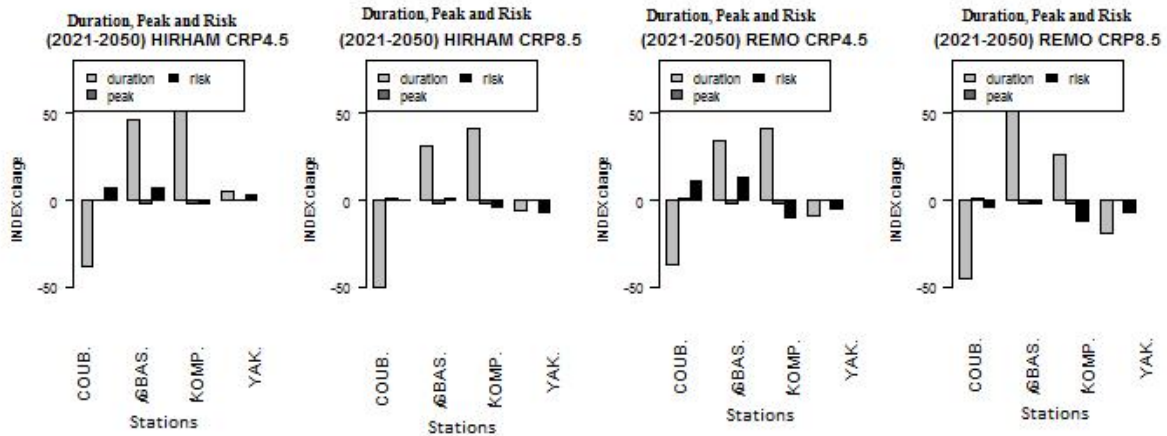


Figure 19. Changes in drought duration, peak and risk (12-month scale).

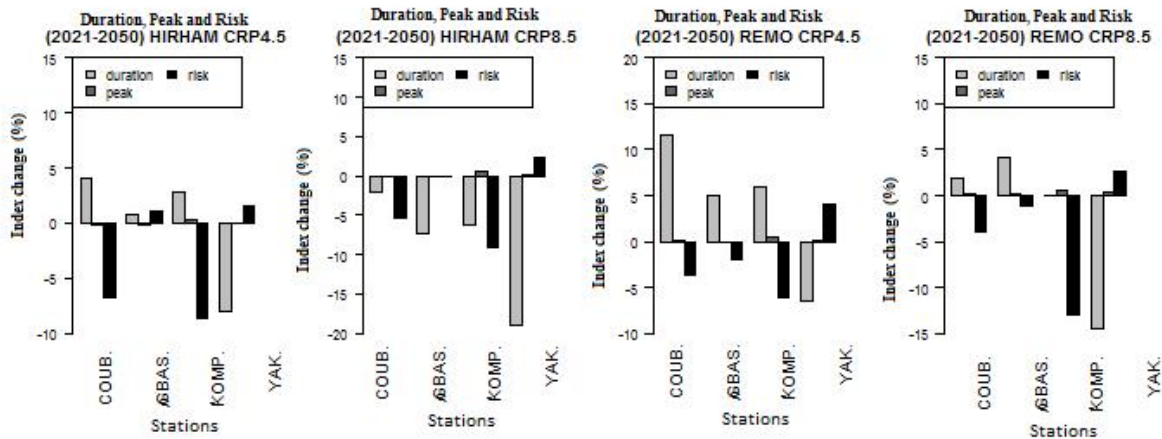


Figure 20. Changes in drought duration, peaks and risks (36-month scale).

with respective peak differences of 0.63, -1.57, -2.03 and -0.03 compared to the reference period. In contrast, its RCP8.5 shows drought duration differences of -45.66, 52, 26 and -18.92 associated with peak differences of 0.89, -1.84, -1.64 and 0.04 respectively at Couberi, Gbassè, Kompongou and Yakin relative to the baseline period (Figure 20).

Drought risk decreases by about 3.01% and 0.62% respectively for the SDI-12 and 36 months under the average of the two model scenarios during the medium term compared to the baseline period (Figures 19 and 20). It should be noted that these obtained changes are not significant as proven with the Student's test ( $p\text{-Value} > 0.05$ ) applied to the indices at 95% confidence level. Whatever the model and the station considered, the Student's  $p\text{-Value}$  is greater than 0.05 (Figure 21).

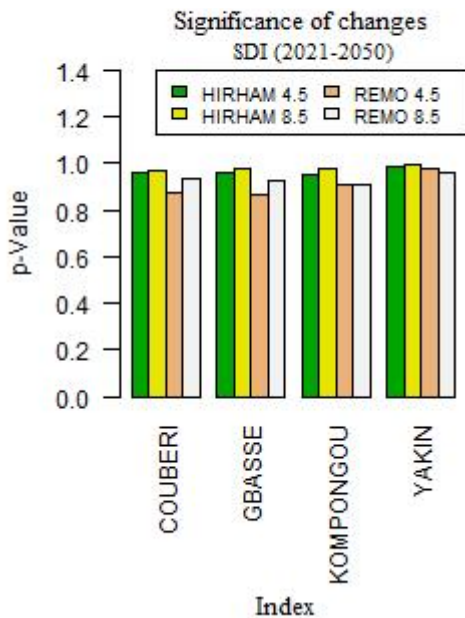


Figure 21. Significance of SDI changes.

#### 4. Discussion

The calculated SDI indices show increasing trends on average for all the model scenarios used. These increases are insignificant (on the order of 0.00001 per year). Therefore, the trends in runoff over the basin will be slightly increasing. This reflects that the wet conditions observed during the baseline period will continue for the next 30 years. Badou<sup>[19]</sup> and Obada<sup>[29]</sup> described many changes for the rivers in the Benin River basin as is also the case with Zhao<sup>[33]</sup> for North America. Also, Koudamiloro<sup>[34]</sup>, also show that the Oueme to Bétérrou watershed in Benin is characterized by droughts to varying degrees. Indeed, hydrological droughts are likely to increase by about 0.0003% over the future period. These variations in

droughts will be accompanied by an increase in their duration and a decrease in their magnitudes (peaks) as shown by all the climate models used. These results corroborate those obtained with several models of the CORDEX program used for many regions of the Arctic, Antarctic and Sahara by Spinoni<sup>[35]</sup>.

On average, there is a slight increase in drought classes. These increases in drought will be followed by increases in drought duration and decreases in drought intensity (peak). These results are obtained in other regions of the world such as Senegal where runoff is expected to increase in the south and decrease in the north according to Moustapha<sup>[36]</sup>. Over the Kentucky basin, Somsubhra<sup>[37]</sup> showed decreases for hydrological drought intensities and increases in their duration. Zhao<sup>[33]</sup>, on the other hand, predict drought duration of future periods to be longer than the historical period. For Zhao<sup>[38]</sup>, future changes in extreme hydrological droughts are very dramatic and will be more severe than meteorological droughts. For all the SDI indices, we notice that the number of dry months increases with the index window, these results affirm those of Ghenim and Megnounif<sup>[39]</sup> for Northwest Algeria through the SPI and SSFI indices.

#### 5. Conclusions

The calculated SDI indices show overall increasing trends during the historical period as well as in the projections. These increases are not significant and evolve in the same direction as precipitation, leading to a slight increase in runoff in the basin. The duration of droughts is also expected to increase, followed by a decrease in their intensity (peak). The basin will therefore experience more dry months but with low incidence. It is also important to note that the changes obtained are not significant at the Student's t test at the 95% level.

#### Conflict of Interest

There is no conflict of interest.

#### References

- [1] Soubeyroux, J.M., Vidal, P.P., Baillon, M., et al., 2010. Characterization and forecasting of droughts and low water levels in France from the Saffron-Isba-Moscow hydrometeorological chain. The White Coal. 5,10. (In French)
- [2] Serhat, S., Necla, T., Alper, A., et al., 2013. Trends in turkey climate indices from 1960 to 2010, 6th Atmospheric Science Symposium, Turkey. pp. 24-26.
- [3] Zengchao, H., Amir, A., Navid, N., et al., 2014. Global integrated drought monitoring and prediction

- system, scientific data. Subject Categories. Water resources. Hydrology. pp. 10.
- [4] Giguère, M., Gosselin, P., 2006. Water and Health: A review of current climate change adaptation initiatives in Quebec. pp. 28. (In French)
- [5] Gnanglè, C.P., Romain, G.K., Achille, E.A., et al., 2011. Past climate trends, modeling, perceptions and local adaptations in Benin. *Climatology*. 8, 14. (In French)
- [6] Heim, R.R.Jr., Brewer, M.J., 2012. The global drought monitor portal: The foundation for a global drought information system. *Earth Interactions*. 16, 1-28.
- [7] Layelmam, M., 2008. Calculation of drought indicators from NOAA/AVHRR images, Drought Early Warning System Project in three countries on the southern shore of the Mediterranean: Algeria, Morocco, and Tunisia LIFE05 TCY/TN/000150. pp. 38. (In French)
- [8] FAO, 1998. Crop Evaporation - Guidelines for computing crop water requirements. Irrigation and Drainage paper; Rome (Italy). 56, <http://www.fao.org/docrep/X0490E/X0490E00.htm>.
- [9] McKee, T.B., Doesken, N.J., Kleist, J., 1993. The relationship of drought frequency and duration at time scales. Eighth Conference on Applied Climatology, American Meteorological Society. Anaheim CA. pp. 179-186.
- [10] OMM, 2006. Drought monitoring, progress and future challenges. (In French)
- [11] Spinoni, J., Naumann, G., Carrao, H., et al., 2013. World drought frequency, duration, and severity for 1951-2010. *International Journal of Climatology*. 34, 2792-2804.
- [12] Oguntundé, G.P., Lischeid, G., Abiodun, J.B. et al., 2016. Analysis of long-term dry and wet conditions over Nigeria, *Journal international de climatologie*. 37(9).
- [13] Ozer, P., Ousmane, L.M., Adamou, D.T., et al., 2017. Recent evolution of rainfall extremes in Niger (1950-2014). *Geo-Eco-Trop.*, 41, 3, n.s., 375-383. Special issue, 10. (In French)
- [14] Batablinle, L., Lawin, A.E., Celestin, M., 2019. Future extremes temperature and rainfall : trends and changes assessment over the mono river basin in west Africa, XXXII AIC International Colloquium, Thessaloniki - Greece. pp. 9-14.
- [15] Kodja, D.J., Batablinle, L., Akognongbe, A., et al., 2019. Rainfall and temperature changes in Oueme watershed by 2080 in west Africa, XXXII AIC International Colloquium, Thessaloniki - Greece.
- [16] Mahé, G., Lienou, G., Bamba, F., et al., 2011. The Niger River and climate change over the last 100 years, *Hydro-climatology: Variability and Change. Proceedings of symposium J-H02 held during IUGG2011 in Melbourne, Australia*. pp. 7. (In French)
- [17] Ozer, P., Hountondji, Y.C., Niang, A.J., et al., 2010. Desertification in the Sahel: history and perspectives. *Bulletin of the Geographical Society of Liege*. 54, 69-84. (In French)
- [18] Vissin, E.W., 2007. Impact de la variabilité climatique et de la dynamique des états de surface sur les écoulements du bassin béninois du fleuve Niger, PhD thesis. pp. 310. (In French)
- [19] Badou, F.D., 2016. Multi-model evaluation of blue and green water availability under climate change in four-non Sahelian basins of the Niger river basin, PhD thesis, University of Abomey-Calavi (UAC), National Water Institute (INE). pp. 155. (In French)
- [20] Christensen, J.H., Hewitson, B., Busuioc, A., et al., 2006. Regional Climate Projections. In: *Climate Change 2007: The physical Sciences Basis. Contribution of Working Group I to the Fourth Assessment Report of the Intergovernmental Panel on Climate Change*, Solomon S, Qin D, Manning M, Chen Z, Marquis M, Averyt KB, Tignor M and HL Miller (eds.) Cambridge University Press: Cambridge, New York. pp. 847-940. <https://www.ipcc-wg1.unibe.ch/publications/wg1-ar4/ar4-wg1-chapter11.pdf>.
- [21] Jacob, D., Bärring, L., Christensen, O.B., et al., 2007. An inter-comparison of regional climate models for Europe: design of the experiments and model performance. *Climatic Change*. 81, 31-52.
- [22] Nalbantis, I., Tsakiris, G., 2008. Assessment of hydrological drought revisited. *Water Resources Management*. 23(5), 881-897.
- [23] Graham, L.P., Andreasson, J., Carlsson, B., 2007. Assessing climate change impacts on hydrology from an ensemble of regional climate models, model scales and linking methods—A case study on the Lule River basin. *Climatic Change*. 81(S1), 293-307.
- [24] Moore, K., Pierson, D., Pettersso, K., et al., 2008. Effects of warmer world scenarios on hydrologic inputs to Lake Mälaren, Sweden and implications for nutrient loads. *Hydrobiologia*. 599, 191-199.
- [25] Sperna, F.C., Van Beek, L.P.H., Kwadijk, J.C.J., et al., 2010. The ability of a GCM-forced hydrological model to reproduce global discharge variability. *Hydrology and Earth System Sciences*. 14(8), 1595-1621.
- [26] Lafon, T., Dadson, S., Buys, G., et al., 2013. Bias cor-

- rection of daily precipitation simulated by a regional climate model: a comparison of methods. *International Journal of Climatology*. 33(6), 1367-1381.
- [27] Allen, R.G., Pereira, L., Raes, D., et al., 1998. Crop evapotranspiration - Guidelines for computing crop waters requirements - FAO irrigation and drainage paper 56; chapters 1, 2, 3 & 4, annex 3 & 5. (<https://www.fao.org/docrep/x0490E/x0490e00.htm>)
- [28] Gaba, O.U.C., Biao, I.E., Alamou, A.E., et al., 2015. An Ensemble Approach Modelling to Assess Water Resources in the Mékrou Basin, Benin. *Hydrology*. 3(2), 22-32.  
DOI: <https://doi.org/10.11648/j.hyd.20150302.11>
- [29] Obada, E., 2017. Approche de quantification des changements récents et futurs de quelques paramètres hydro-climatiques dans le bassin de la Mékrou (Bénin), Université d'Abomey-Calavi (Bénin), PhD Thesis. pp. 212. (In French)
- [30] Afouda, A., Lawin, E., Lebel, Th., 2004. A stochastic Streamflow Model based on Minimum Energy Expenditure Concept. In contemporary Problems in Mathematical Physics: Proceeding 3rd Intern. Workshop. Word Scientific Publishing Co. Ltd. pp. 153-169.
- [31] Alamou, E., 2011. Application of the Least Action Principle to Rainfall-Flow Modelling, PhD thesis, University of Abomey Calavi, 231 pages & Appendices. (In French)
- [32] Afouda, A., Alamou, E., 2010. Hydrological model based on the principle of least action (MODHYPMA). *Annals of Agronomic Sciences of Benin*. (In French)
- [33] Zhao, C., Brissette, F., Chen, J., et al., 2019. Frequency change of future extreme summer meteorological and hydrological droughts over North America. *Journal of Hydrology*. pp. 11.
- [34] Koudamilo, O., Vissin, E.W., Sintondji, L.O., et al., 2015. Socio-economic and environmental effects of hydroclimatic hazards in the Oueme River watershed at the outlet of Bétéro in Benin (West Africa), XXVIIIth Colloquium of the International Association of Climatology, Liège. pp. 6. (In French)
- [35] Spinoni, J., Paulo, B., Edoardo, B., et al., 2020. Future Global Meteorological Drought Hot Spots: A Study Based on CORDEX Data. *Journal of Climate*. pp. 27.
- [36] Moustapha, T., Mouhamadou, B.S., Ismaïla, D., et al., 2017. Projected impact of climate change in the hydroclimatology of Senegal with a focus over the Lake of Guiers for the twenty-first century. *Theoretical & Applied Climatology*. 129, 655-665.  
DOI: <https://doi.org/10.1007/s00704-016-1805-y>
- [37] Somsubhra, C., Dwayne, R.E., Yao, Y., et al., 2017. An Assessment of Climate Change Impacts on Future Water Availability and Droughts in the Kentucky River Basin. *Environment Process*. pp. 30.
- [38] Zhao, C., Brissette, F., Chen, J., et al., 2020. Evolution of future extreme drought frequency in two climate model large ensembles, EGU General Assembly 2020, Online. EGU2020-11449.  
DOI: <https://doi.org/10.5194/egusphere-egu2020-11449>
- [39] Ghenim, A.N., Megnounif, A., 2011. Characterization of the drought by the SPI and SSFI indices (northwest Algeria), *Scientific and Technical Review, LJEE*. 18, 20. (In French)